

Tracking the Cheetah Tail using Animal-Borne Cameras, GPS and an IMU

Amir Patel^{1**}, Bradley Stocks¹, Callen Fisher^{1*}, Fred Nicolls^{1**} and Edward Boje^{1**}

¹ Department of Electrical Engineering, University of Cape Town, Cape Town, 7700, South Africa

* Student Member, IEEE

** Member, IEEE

Abstract— The cheetah (*Acinonyx Jubatus*) is the fastest terrestrial animal and is also highly maneuverable. An investigation into the whole-body motion dynamics of this specialized predator will illuminate various factors that influence and affect performance in legged animals as well as provide insight for the design of future bio-inspired robots. Presently, animal sensor collars can capture the gross animal behavior successfully, but do not provide information about the animal's complete motion. Here, in an effort towards whole-body motion estimation, we demonstrate the use of animal mounted cameras, as well as the sensor suite of a smartphone which are attached to captive cheetahs during maneuvers. The various sensors are fused by an Extended Kalman Smoother to provide high-bandwidth state estimates of the position, velocity and acceleration of the cheetah spine and tail.

Index Terms—animal tracking, cheetah, Kalman smoother, multi-sensor data fusion, IMU

I. INTRODUCTION

We seek to understand the locomotion of the cheetah, whose success in hunting has been attributed to its maneuverability [1]. However, the use of the spine and tail, which appear to be crucial to the cheetah's dexterity, have not fully been analyzed. Indeed, studies have shown that the cheetah tail possesses aerodynamic effects [2] and that wheeled robots which emulate the tail motions can increase their acceleration performance [3] [4]. But deeper insight necessitates the capture of high-fidelity multibody kinematic data from live cheetahs. Insight obtained may be relevant to the design of the next generation of agile, bio-inspired robots.

Obtaining this type data from free-running animals is challenging. Biomechanists regularly use stationary cameras for studying animal kinematics and have done so to investigate steady-state galloping in cheetahs [5]. This method is limited to a fixed capture area and as such would not be suitable for transient (non-steady) maneuvers which are often unplanned. Additionally, they require multiple calibrated cameras as well as time synchronization.

Other researchers have opted for the use of animal-borne cameras to circumvent this problem to study the hunting strategies of falcons [6] and swimming in marine mammals [7]. However, the most popular method for studying free-running animals is tracking collars, which employ the use of a Global Positional System (GPS) sensor, inertial measurement unit (IMU) or magnetometer combination [1] [8] [9]. This approach has a theoretically infinite capture volume but is unable to capture the multibody kinematics of the animal.

Here, we present a novel approach for motion capture of free-running cheetahs which utilizes two animal-borne cameras, GPS sensor, pressure sensor and a 9-axis IMU, conveniently packaged in a smartphone for this initial investigation. This approach was tested as a proof-of-principle using off the shelf components on captive

cheetahs. The various sensors were fused by an Extended Kalman Smoother (EKS) to provide high-fidelity kinematic estimates of the spine and tail as shown in Fig. 1. The use of animal-attached sensors and multi-sensor fusion proposed here has the potential to enhance studies of biomechanics and maneuverability on free-ranging animals.



Fig. 1: Image of a tail flick taken from one of the animal-borne cameras.

II. MOTION CAPTURE SYSTEM

In this study, we combined the advantages of GPS/IMU tracking collars with those of animal-borne cameras. However, unlike [6] we aimed the cameras towards the rear of the animal to capture the motion of its spine and tail. Key points were then tracked and a multibody kinematic model is utilized for state estimation as described in Section III.

A. Hardware

Using their IMU and GPS sensors, smartphones have been shown to provide considerable accuracy for attitude estimation [10]. As such, we elected to use the Sony Xperia Z3 Mini (weight 106 g) which contains a GPS, IMU (3-axes gyro, accelerometer and magnetometer)

Corresponding author: A. Patel (a.patel@uct.ac.za).

1949-307X © 2016 IEEE. Personal use is permitted, but republication/redistribution requires IEEE permission.

See http://www.ieee.org/publications_standards/publications/rights/index.html for more information. (Inserted by IEEE)

and a barometric pressure sensor. For the animal-borne cameras, the GoPro Hero Session was chosen as it is lightweight (74 g) and is capable of 720p resolution video at 100 frames per second. The system employed two of these cameras for stereo vision. For the proof-of-principle test on captive cheetahs, a GoPro Fetch canine harness was modified with a 3D printed holder for the cameras and smartphone, and is depicted in Fig. 2.

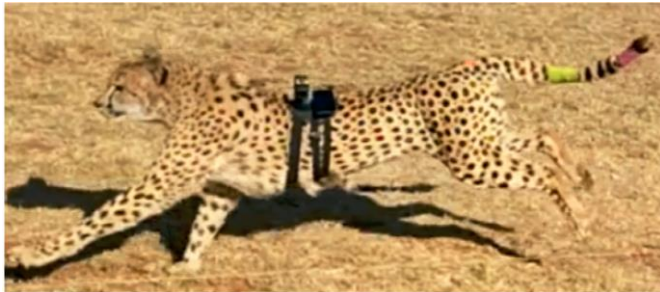


Fig. 2: A GoPro Fetch harness was modified and used for attachment of sensors to the cheetahs. Colored markers were also attached to the tail and base of the spine.

B. Software

An Android application was written for the phone and its primary tasks were to:

- Log sensor data from the phone at 100 Hz.
- Synchronize the camera and phone data by using a beep sound at the start/stop of logging.

To facilitate feature detection, colored bands were placed on the base of the spine (orange), middle of the tail (green) and tip of the tail (pink). A Matlab script was written to detect each color in a semi-supervised manner and the two cameras were calibrated for intrinsics and extrinsics using the Matlab camera calibration toolbox.

Temperature bias calibration of the gyro and accelerometer was performed, as well as magnetometer calibration against soft and hard iron effects. All estimation and calibration was done in Matlab.

III. STATE ESTIMATION

A. Kinematic Model

To estimate the motion of the cheetah, the spine and tail were modelled as a kinematic chain consisting of 4 rigid links as shown in Fig. 3 based on previous work [2]. The position of the end of each of the links (2-4) relative to the inertial frame can be generally described as,

$$\mathbf{p}_i^0 = \mathbf{p}_{i-1}^0 + \mathbf{R}_i^0 \begin{pmatrix} L_i \\ 0 \\ 0 \end{pmatrix}, \quad (1)$$

where \mathbf{R}_i^0 rotates a vector from frame i to the inertial frame (0); L_i represents the length of the link i ; and \mathbf{p}_{i-1}^0 is the position of the previous link. We express these rotation matrices as Euler angles (roll – φ_i , pitch – θ_i , yaw – ψ_i) such that:

- Link 1 (L_1 – the collar): translates ($\mathbf{p}_1^I = [x, y, z]^T$) and rotates (Euler 3-2-1) relative to the inertial frame
- Link 2 (L_2 – back of the spine): for simplicity, we only allow to rotate in the pitch axis (θ_2) relative to Link 1

- Link 3 (L_3): rotates in the pitch axis (θ_3) and then rotates in the yaw axis (ψ_3) relative to Link 2
- Link 4 (L_4): rotates in the pitch axis (θ_4) and then rotates in the yaw axis (ψ_4) relative to Link 3.

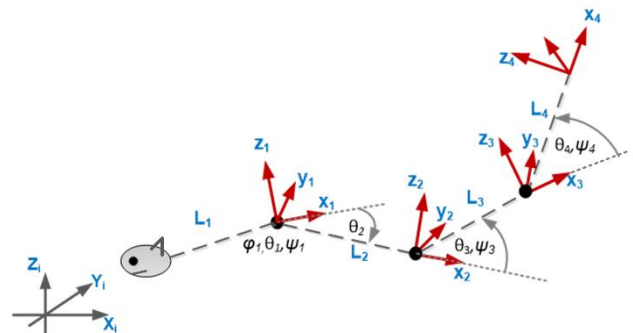


Fig. 3: The cheetah is modelled as a kinematic chain consisting of 4 rigid links. The markers (orange, green and pink) are located at the ends of links 2, 3 and 4 respectively.

B. Measurements

The system consists of several sensors which are sampled at various rates, summarized in Table 1. The marker measurements are asynchronous and are only available when the marker is not occluded. The measurement equations for the accelerometer, gyro and magnetometer are respectively expressed as,

$$\begin{aligned} \mathbf{z}_{acc} &= \mathbf{R}_0^1 \left(\ddot{\mathbf{p}}_1^0 - \begin{bmatrix} 0 \\ 0 \\ g \end{bmatrix} \right) \\ \mathbf{z}_{gyro} &= \mathbf{R}_\omega^1 \boldsymbol{\omega}_1^0 \\ \mathbf{z}_{mag} &= \mathbf{R}_0^1 \mathbf{m}_1^0, \end{aligned} \quad (2)$$

where g is the gravitational constant, \mathbf{R}_ω^1 rotates the total angular velocity of Link 1 in the inertial frame ($\boldsymbol{\omega}_1^0$) into Link 1's frame and \mathbf{m}_1^0 is the local magnetic vector expressed in the inertial frame. The GPS measurements provide the inertial position, velocity and heading, while the pressure measurement equation is based on the barometric formula for altitude [11].

Table 1: Various data rates of the sensors are shown.

Sensor	Measurement Units	Data Rate
3D Accelerometer	m/s ²	100 Hz
3D Gyro	rad/s	100 Hz
3D Magnetometer	Gauss	100 Hz
Pressure Sensor	Pa	4 Hz
2D GPS Position	m	1 Hz
2D GPS Speed	m/s	1 Hz
GPS Heading	deg	1 Hz
Camera 1 (Orange)		
Camera 2 (Orange)		
Camera 1 (Pink)	2D pixel position	As detected
Camera 2 (Pink)		
Camera 1 (Green)		
Camera 2 (Green)		

Each camera measurement of a marker (a) relative to the camera in Link 1's frame (\mathbf{p}_{1a}^1) is individually expressed for each camera's

image plane (in pixels) using its perspective projection matrix \mathbf{C} as [12]

$$\mathbf{z}_{m_a} = \begin{bmatrix} \mathbf{c}_1 \\ \mathbf{c}_2 \end{bmatrix} \begin{bmatrix} \mathbf{p}_{m_a}^1 \\ 1 \end{bmatrix} \left(\mathbf{c}_3 \begin{bmatrix} \mathbf{p}_{m_a}^1 \\ 1 \end{bmatrix} \right)^{-1} \quad (3)$$

where \mathbf{c}_b is row \mathbf{b} of \mathbf{C} .

C. Extended Kalman Smoother

The kinematic states of the links (position, velocity and acceleration) were estimated, with the position vector expressed as:

$$\mathbf{q} = [x \ y \ z \ \varphi_1 \ \theta_1 \ \psi_1 \ \theta_2 \ \theta_3 \ \psi_3 \ \theta_4 \ \psi_4]^T. \quad (4)$$

For the purposes of the filter, the system was modelled as having constant acceleration corrupted with noise covariance accounting for jerk. The motion of the animal is periodic while running, therefore, to aid estimation, the base of the spine (Link 2) was modelled as an oscillator with unknown frequency (K , to model the first harmonic) and bias (B) as additional state variables. This resulted in a state vector

$$\mathbf{X} = [\ddot{\mathbf{q}} \ \dot{\mathbf{q}} \ \mathbf{q} \ K \ B]^T. \quad (5)$$

To track the state variables (35 in total) adequately, an EKS was employed [13]. This consists of a forward pass Extended Kalman Filter (EKF), followed by a backward recursive smoothing algorithm to produce the smoothed state estimate ($\tilde{\mathbf{x}}_k^S$) and covariance (\mathbf{P}_k^S) described by the following¹:

$$\begin{aligned} \mathbf{A}_k &= \mathbf{P}_k \mathbf{F}_k^T [\mathbf{P}_k^-]^{-1} \\ \tilde{\mathbf{x}}_k^S &= \tilde{\mathbf{x}}_k + \mathbf{A}_k (\tilde{\mathbf{x}}_{k+1}^S - \tilde{\mathbf{x}}_{k+1}^-) \\ \mathbf{P}_k^S &= \mathbf{P}_k + \mathbf{A}_k (\mathbf{P}_{k+1}^S - \mathbf{P}_{k+1}^-) \mathbf{A}_k^T \\ k &= N - 1, \dots, 0 \end{aligned} \quad (6)$$

where \mathbf{F} is the state transition matrix, \mathbf{A} is the smoother gain matrix, N is the final step, $\tilde{\mathbf{x}}_k^-$ and \mathbf{P}_k^- are the predicted mean and covariance of the state, $\tilde{\mathbf{x}}_k$ and \mathbf{P}_k are the estimated mean and covariance of the state vector, respectively at time step, k . The algorithm was executed at 100 Hz.

To tune the filter, the covariances of the first derivative of the accelerometer and the second derivative of the gyro were used as estimates for the noise covariance on the acceleration states. For the measurement covariance estimates, the smartphone sensors' variance was measured while the phone was kept stationary. The camera was calculated to track the markers within 5 pixels.

After initial analysis, it was discovered that the tail angles tended to drift when the tail markers were not seen. However, wildlife footage and our stationary test footage indicated that the tail tended to be kept straight out backwards when not being swung actively. To account for this, a noisy pseudo-measurement (0° , $\sigma = 30^\circ$) was introduced whenever the markers were not detected.

IV. EXPERIMENTS

The system was tested on three adult cheetahs at the Ann van Dyk Cheetah Centre (Pretoria, South Africa)². Data was collected during the animal's weekly exercise runs where they would chase a lure attached to a pulley-winch system. Standard EKF and EKS methods were used to estimate state vectors. An example of results for one of the cheetah runs is shown in Fig. 4A where the animal ran one way (to $(x, y) = [-100, -40]$ m) and then turned around sharply and ran back to the origin after approximately 9 s (sample 900). This sharp turn is noted by the estimates of the roll angle and corresponding heading angle change.

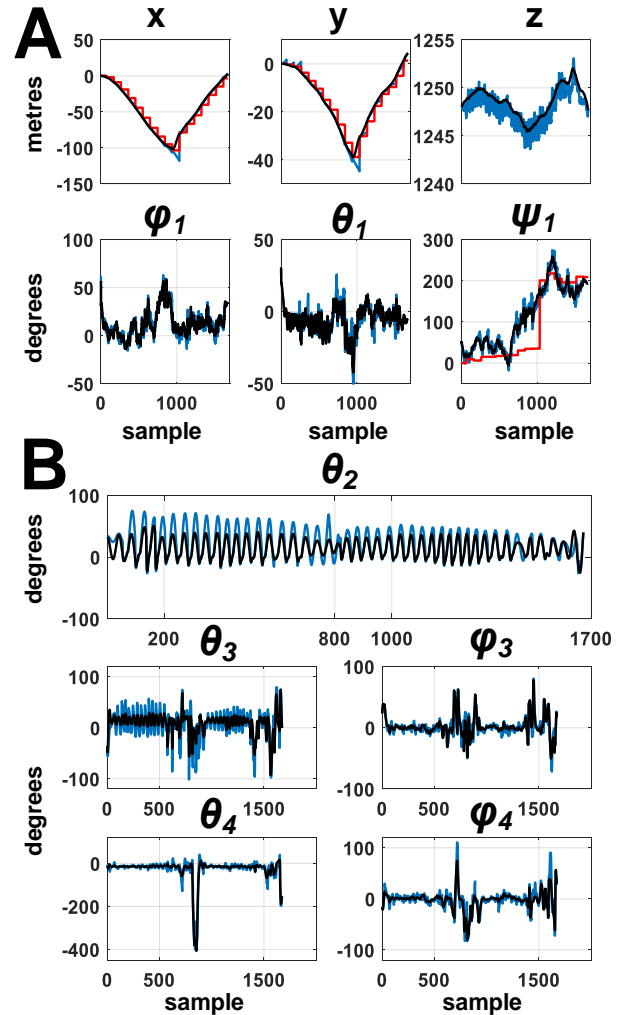


Fig. 4: (A) Link 1 position and attitude estimates are shown. Blue, Black and Red represents EKF, EKS and GPS data respectively. (B) The spine and tail angles are tracked throughout the entire run.

As seen in Fig. 4A, the combination of measurements and assumed dynamic model results in tracking of the gross motion of the animal as well as the periodic spine motion. This periodic behavior is compatible with the video observations. Lastly, as illustrated in Fig. 5, the system can track the high-speed tail flicks.

¹ For the sake of brevity, we have not included the EKF algorithm equations. For more information, see [13].

² Ethics approval was obtained from the University of Cape Town Health Science Faculty Animal Ethics Committee

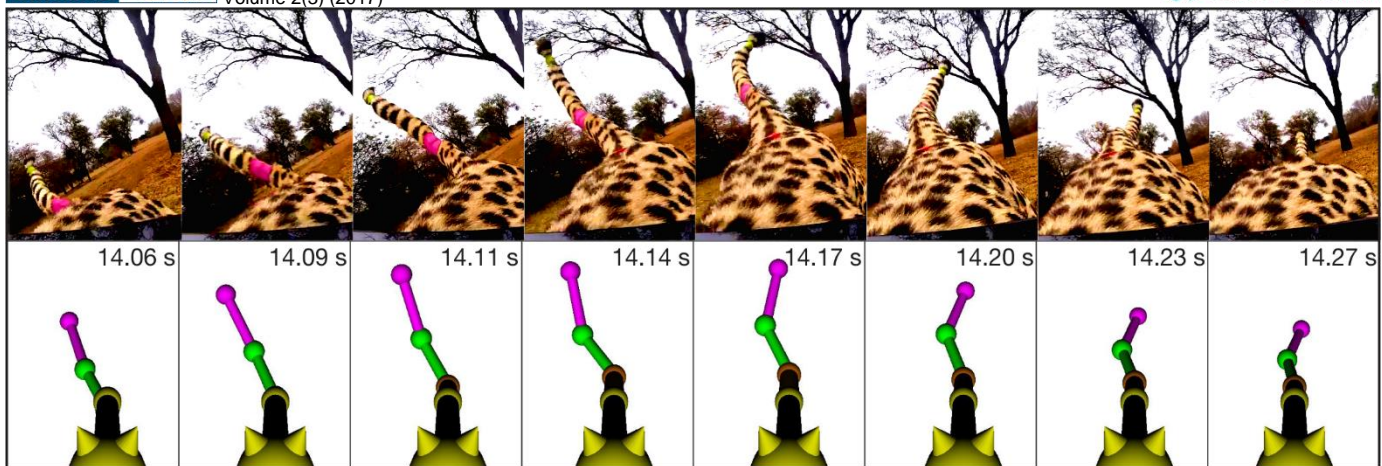


Fig. 5: Example of a high-speed tail flick tracked by the EKS algorithm is shown above and compared to the camera footage.

V. CONCLUSION & FUTURE WORK

By combining the advantages of GPS/IMU collars and animal-borne cameras, we can track the detailed motion of the cheetah multibody kinematics without the need for external cameras.

This approach could enable biomechanics studies of maneuverability in not only the cheetah but free-running animals in general. There are two avenues for future work:

- For this approach to be applicable for tracking free ranging animals, size, weight, power and cost (SWap-C) must be considered. This can be achieved by designing a bespoke embedded system with a photovoltaic panel for power harvesting as done in previous studies [1] [8]. The system would require a wireless link for the download of data, as well software to put the system into a low power mode when the animal is stationary and then wake it up when activity is detected [1]. Even though a harness offers better stability on the animal, it may be impractical to mount on a wild animal, thus a collar based system should be considered. The GoPro cameras could be replaced by miniature camcorders embedded in the collar as done in [6].
- Secondly, to obtain the motion of the limbs, wireless IMUs (e.g. *XSens* or *Notch* sensors), could be attached to legs in various positions as done in equine limb studies [14]. This would allow the complete body (limbs, spine and tail) kinematics of the animal to be estimated through fusing a more detailed model (additional links for each limb) with additional measurement equations and the animal-borne camera data.

ACKNOWLEDGMENT

The authors would like to thank Rita Groenewald and the team at the Ann van Dyk Cheetah Centre as well as Zayaan Majiet at the K9 Training Centre and Kennels. We would also like to thank Stacey Shield for assistance with graphics and A/Prof Andrew Markham for initial discussions. This work was partially supported by the National Research Foundation (NRF) of South Africa under Grant 99380 as well as the Claude Leon Foundation.

REFERENCES

- [1] A. Wilson, J. Lowe, K. Roskilly, P. Hudson, K. Golabek and K. McNutt, "Locomotion dynamics of hunting in wild cheetahs," *Nature*, vol. 498, pp. 185-189, 2013.
- [2] A. Patel, E. Boje, C. Fisher, L. Louis and E. Lane, "On the Aerodynamics of the Cheetah Tail," *Biology Open*, vol. 5, no. 8, pp. 1072-1076, 2016.
- [3] A. Patel and E. Boje, "On the Conical Motion of a Two-Degree-of-Freedom Tail Inspired by the Cheetah," *IEEE Transactions on Robotics*, vol. 31, no. 6, pp. 1555-1560, 2015.
- [4] A. Patel and M. Braae, "Rapid Acceleration and Braking: Inspirations from the Cheetah's Tail," in *IEEE International Conference on Robotics and Automation*, Hong Kong, 2014.
- [5] P. Hudson, S. Corr and A. Wilson, "High speed galloping in the cheetah (*Acinonyx jubatus*) and the racing greyhound (*Canis familiaris*): spatio-temporal and kinetic characteristics.," *Journal of Experimental Biology*, vol. 215, no. 14, pp. 2425-2434, 2012.
- [6] S. A. Kane and M. Zamani, "Falcons pursue prey using visual motion cues: new perspectives from animal-borne cameras," *Journal of Experimental Biology*, vol. 217, no. 2, pp. 225-234, 2014.
- [7] T. Williams, R. Davis, L. Fuiman, J. Francis, B. Le, M. Horning, J. Calambokidis and D. Croll, "Sink or swim: strategies for cost-efficient diving by marine mammals," *Science*, vol. 288, no. 5463, pp. 133-136, 2000.
- [8] J. W. Wilson, M. G. Mills, R. P. Wilson, G. Peters, M. E. Mills, J. R. Speakman and M. Scantlebury, "Cheetahs, *Acinonyx jubatus*, balance turn capacity with pace when chasing prey," *Biology Letters*, vol. 9, no. 5, September 2013.
- [9] A. Markham, N. Trigoni, D. Macdonald and S. Ellwood, "Underground localization in 3-D using magneto-inductive tracking," *IEEE Sensors Journal*, vol. 12, no. 6, pp. 1089-1816, 2012.
- [10] J. Gośliński, M. Nowicki and P. Skrzypczyński, "Performance comparison of EKF-based algorithms for orientation estimation on Android platform," *IEEE Sensors Journal*, vol. 15, no. 7, pp. 3781-3792, 2015.
- [11] A. Sabatini and V. Genovese, "A sensor fusion method for tracking vertical velocity and height based on inertial and barometric altimeter measurements," *Sensors*, vol. 14, no. 8, pp. 13324-13347, 2014.
- [12] R. Hartley and A. Zisserman, *Multiple View Geometry in Computer Vision*, Cambridge University Press, 2004.
- [13] W. Chan and F. Hsiao, "Implementation of the Rauch-Tung-Striebel smoother for sensor compatibility correction of a fixed-wing unmanned air vehicle," *Sensors*, vol. 11, no. 4, pp. 3738-3764, 2011.
- [14] E. Olsen, P. Haubro Andersen and T. Pfau, "Accuracy and precision of equine gait event detection during walking with limb and trunk mounted inertial sensors," *Sensors*, vol. 6, no. 8, pp. 8145-8156, p. 12, 2012.